Captan-induced increase in the concentrations of intracellular Ca^{2+} and Zn^{2+} and its correlation with oxidative stress in rat thymic lymphocytes

Tomomi Inoue[1,*], Maika Kinoshita[1,*], Keisuke Oyama[2], Norio Kamemura[3], Yasuo Oyama[1]

[1] Faculty of Bioscience and Bioindustry, Tokushima University, Tokushima 770-8513, Japan

[2] Sakai City Medical Center, Sakai 593-8304, Japan

[3] Faculty of Life Sciences, Tokushima Bunri University, Tokushima 770-8514, Japan

[*] These authors equally contributed to this research.

Corresponding author: Yasuo Oyama, Ph.D.

E-mail: oyamay@tokushima-u.ac.jp

Tel: 81-88-656-7256

Abstract

Captan, a phthalimide fungicide, is considered to be relatively nontoxic to mammals. There is a possibility that captan affects membrane and cellular parameters of mammalian cells, resulting in adverse effects, because of high residue levels. To test the possibility, we examined the effects of captan on rat thymic lymphocytes using flow-cytometry with appropriate fluorescent probes. Treatment with 10 and 30 μM captan induced apoptotic and necrotic cell death. Before cell death occurred, captan elevated the intracellular concentrations of Ca^{2+} and Zn^{2+} and decreased the concentration of cellular thiol compounds. These captan-induced phenomena are shown to cause cell death and are similar to those caused by oxidative stress. Captan also elevated the cytotoxicity of hydrogen peroxide. Results indicate that 10 and 30 μM captan cause cytotoxic effects on mammalian cells. Despite no report on the significant environmental toxicity hazard of captan in humans, it may exhibit adverse effects, described above, on wild organisms.

Keywords: Captan; Intracellular Ca^{2+}; Intracellular Zn^{2+}; Nonprotein thiols; Superoxide anions; Lymphocytes

Highlights

• Captan at sublethal levels induces adverse effects on rat lymphocytes.

• Captan raises intracellular Ca^{2+} level by increasing membrane Ca^{2+} permeability.

• Captan raises intracellular Zn^{2+} level by increasing intracellular Zn^{2+} release.

• Captan raises and lowers cellular thiol content as captan concentration increases.

• Captan increases cell vulnerability to oxidative stress.

1. Introduction

Captan is a broad-spectrum phthalimide fungicide used to control fungal diseases in grapes and orchards (DeMarsay, 2012; Abbott and Beckerman, 2018). Annual agricultural use of captan in the USA was estimated to be about 3 million pounds during the last decade (Pesticide National Synthesis Project, US Geological Survey, 2018). Its main antifungal mechanism is to irreversibly react with endogenous substances containing thiol groups, resulting in an overall reduction of several fungal enzymatic activities (Arce et al., 2010; Lukens, 2013). This mechanism may be involved in the toxicity of captan against other organisms including mammals because the hepatotoxicity of captan on rats appears to be reduced by prior administration of glutathione, a sulfhydryl-containing compound (Dalvi, 1988). Captan increased cellular parameters for oxidative damages in isolated rat hepatocytes (Suzuki et al., 2004). It is therefore thought that the reduction of nonprotein thiols by captan augments the oxidative stress in nontarget microorganisms and mammalian cells. Captan induces necrotic and apoptotic cell death in nontarget microorganisms (Scariot et al., 2017). If captan causes strong oxidative stress in non-target organisms, it would induce various cellular actions that are linked with cell death. Excessive elevations of intracellular Ca^{2+} and Zn^{2+} levels are associated with cell death caused by cytotoxic chemicals (Kawanai et al., 2009; Hashimoto et al., 2009; Bhosale et al., 2015; Slepchenko et al., 2017). Since the homeostasis of intracellular Zn^{2+} is partly controlled by cellular thiols that complex with Zn^{2+} (Maret, 1994; Kocyła et al., 2018), it is possible that captan also affects intracellular Zn^{2+} levels. However, there is limited information regarding the captan-induced changes in intracellular Ca^{2+} and Zn^{2+} concentrations. Thus, we examined the effects of captan on intracellular Ca^{2+} and Zn^{2+} concentrations of rat

thymic lymphocytes using a flow cytometric technique with appropriate fluorescent probes. This study also provides a few insights on the impact of captan as an environmental pollutant on human and wild mammals because if captan exhibits adverse effects on thymic lymphocytes, an immunotoxic effect may result in neonates and adolescents, as the thymus is most active during those periods in mammalian lives.

2. Materials and methods

2.1. Chemicals

Phthalimide fungicides (captan, captafol, and folpet) with > 99.5 % purities were purchased from Tokyo Chemical Industry Co., Ltd. (Tokyo, Japan). Fluorescent probes used to measure various cellular parameters and specific reagents such as Zn^{2+} chelators are listed in Table 1. Other chemical reagents were obtained from Wako Pure Chemicals (Osaka, Japan) and Dojin Chemicals (Kumamoto, Japan).

(Table 1 near here)

2.2. Cell preparation

The use of (T29-54) experimental animals was approved by the Animal Experiment Committee of Tokushima University (Tokushima, Japan). The thymus glands were dissected from 12 thiopental-anesthetized male Wistar rats (6–12 weeks, Japan Charles River, Shizuoka, Japan), razor-sliced, triturated in Tyrode's solution at 1–4ºC, and buffered with HEPES to obtain a single-cell suspension (Chikahisa et al., 1996). The suspension was passed through a 50 µm filter before use in the experiments. The cells were incubated at 36–37ºC for at least 1 h before each experiment because the cells were isolated under cold conditions.

2.3. Experimental procedures and cytometric measurements

All experiments using the cell suspension were carried out at 36–37ºC. The phthalimide fungicides, dissolved in dimethyl sulfoxide (1–30 mM), were added to the cell suspension to achieve various final concentrations (1–30 μM); 300 μM H_2O_2 was used to induce oxidative stress in the cells. Dimethyl sulfoxide as a solvent at 0.1–0.3% was found not to affect the measurement of cellular parameters including probe fluorescence and cell viability of rat thymic lymphocytes under the present experimental conditions.

Fluorescence analysis was performed using a flow cytometer (CytoACE-150; JASCO, Tokyo, Japan with the JASCO software, Version 3.06). Cell lethality was assessed by adding 5 μM propidium iodide (PI). The cells exhibiting PI fluorescence were assumed to be dead. Exposure of phosphatidylserine on the external surface of cell membrane was determined by FITC fluorescence after cell treatment with annexin V-FITC (10 μL/mL) and propidium iodide (5 μM) for 0.5 h (Koopman et al., 1994). To determine the changes in the intracellular concentrations of nonprotein thiols ([NPT]i), the cells were treated with 500 nM 5-CMF-DA for 0.5 h before the measurement of 5-CMF fluorescence (Chikahisa et al., 1996). Fluo-3-AM and FluoZin-3-AM were used to monitor the changes in the intracellular concentrations of Ca^{2+} ($[Ca^{2+}]i$) (Kao et al., 1996) and Zn^{2+} ($[Zn^{2+}]i$) (Gee et al., 2002), respectively. The cells were treated with 1 μM Fluo-3-AM or FluoZin-3-AM for 1 h before fluorescence measurement. To determine the cellular concentration of superoxide anions ($[O_2^-]i$), the cells were treated with 5 μM BES-SO-AM for 1 h before measuring BES-SO fluorescence (Maeda et al., 2005). Excitation and emission wavelengths for the fluorescent probes are also listed in Table 1.

2.4. Statistical analysis

The data were statistically analyzed using Tukey's multivariate analysis software (Excel Tokei, SSRI, Tokyo, Japan). $P < 0.05$ was considered significant. Experimental values are described as mean ± standard deviation (SD) of four samples. Each experiment was performed twice or thrice to validate the results.

3. Results

3.1. Cytotoxic action of captan

The cells were incubated with 1, 3, 10, and 30 μM captan for 3 h to assess the cytotoxicity (the population of cells exhibiting propidium fluorescence). As shown in the cytograms (forward scatter versus propidium fluorescence) of Figure 1A, the treatment with 30 μM captan greatly increased the population of cells with propidium fluorescence (dead cells). Figure 1B shows the concentration-dependent change in the percentage of dead cell population (cell lethality) induced by 1–30 μM captan. A significant increase in cell lethality was observed in cells treated with 10 and 30 μM captan. The forward scatter of propidium iodide-negative and -positive cells (living and dead cells) was reduced by 30 μM captan (Figure 1A and 1B), indicating that the cytotoxicity of 30 μM captan was associated with cell shrinkage. The side scatter, which reflects the cell density, of cells without propidium fluorescence was increased by the treatment with 10 and 30 μM captan (Figure 1C).

(Figure 1 near here)

3.2. Process of cell death induced by captan

The cells were treated with captan for 1 h and then the cells were further incubated with propidium iodide and annexin V-FITC for 0.5 h to assess the process of cell death. As shown in

Figure 2A, the cell treatment with 30 μM captan, but not with 10 μM, significantly increased the population of cells without propidium fluorescence and with FITC fluorescence (area A of cytogram, annexin V-positive living cells).. The population of cells exhibiting propidium fluorescence (areas P and AP, dead cells) was slightly increased by 30 μM captan. Captan-induced changes in the population of cells classified by propidium iodide and annexin V-FITC are summarized in Figure 2 B.

(Figure 2 near here)

3.3. Captan-induced increase in $[Ca^{2+}]i$

The cells preloaded with Fluo-3-AM were treated with 1–30 μM captan for 1 h to assess the captan-induced change in $[Ca^{2+}]i$ before cell death. As shown in Figure 3A, captan increased the intensity of Fluo-3 fluorescence in a concentration-dependent manner. Significant elevation of $[Ca^{2+}]i$ was observed in cells treated with 10–30 μM captan. Subsequent examination of the effect of captan under external Ca^{2+}-free conditions to reveal the source of Ca^{2+} that contribute to captan-induced elevation of $[Ca^{2+}]i$ showed that captan failed to increase the intensity of Fluo-3 fluorescence (Figure 3B), indicating its dependence on external Ca^{2+}.

(Figure 3 near here)

3.4. Captan-induced increase in $[Zn^{2+}]i$

The effects of 1–30 μM captan were examined on the cells that were preloaded with FluoZin-3-AM to assess the captan-induced change in $[Zn^{2+}]i$. Figure 4A shows that 10–30 μM captan increased the intensity of FluoZin-3 fluorescence in a concentration-dependent manner, indicating the elevation of $[Zn^{2+}]i$. To determine the source of Zn^{2+} that contributes to the captan-induced elevation of $[Zn^{2+}]i$, the effect of captan was examined under external Zn^{2+}-free

conditions that was prepared with DTPA, a chelator for external Zn^{2+}. Captan at 10–30 μM similarly increased the intensity of FluoZin-3 fluorescence under external Zn^{2+}-free conditions, indicating the independence from external Zn^{2+} (Figure 2B). Furthermore, a large amount of captan-induced FluoZin-3 fluorescence disappeared in the cells treated with TPEN, a intracellular Zn^{2+} chelator (Figure 4B).

(Figure 4 near here)

3.5. Captan-induced changes in oxidative stress

The effects of 1–30 μM phthalimide fungicides on the [NPT]i and $[O_2^-]$i were examined. The cells were treated with captan, captafol, or folpet for 1 h and then the cells were incubated with 5-CMF-DA for 0.5 h to assess the captan-induced change in [NPT]i in continued presence of respective fungicide. Total time of treatment with fungicide was 1.5 h. Figure 5A shows the decreases in 5-CMF fluorescence induced by 10 and 30 μM captan, 30 μM captafol, and 30 μM folpet, indicating significant reductions of [NPT]i. When the 5-CMF fluorescence was measured only from living cells (the cells without PI fluorescence), the cell lethalities were 3.6 ± 0.2 % (mean ± SD of four samples) for control, 5.6 ± 0.6 % for 30 μM captan, 7.8 ± 0.3 % for 30 μM captafol, and 5.0 ± 0.5 % for 30 μM folpet. Such slight increases in cell lethalities were statistically significant ($P < 0.01$).

The effects of 10 and 30 μM captan were also examined on the cells that were preloaded with BES-SO-AM to assess the captan-induced change in $[O_2^-]$i. The treatment of cells with captan for 1.5 h significantly increased the intensity of BES-SO fluorescence (Figure 5B), indicating significant increases in $[O_2^-]$i.

(Figure 5 near here)

3.6. Captan-induced increase in cell vulnerability to oxidative stress

A decrease in [NPT]i and an increase in $[Zn^{2+}]i$ may elevate the cytotoxicity of H_2O_2 (Matsui et al., 2010). As shown in Figure 6, the treatment with 3 μM captan for 3 h did not result in the change of the cell lethality. However, the simultaneous treatment of 3 μM captan and 300 μM H_2O_2 resulted in the elevated cytotoxicity of H_2O_2. In addition, 10 μM captan slightly increased the cell lethality (Figures 1B and 6) and greatly elevated the cytotoxicity of H_2O_2 (Figure 6).

(Figure 6 near here)

3.7. Effect of TPEN on the captan-induced cytotoxicity

TPEN significantly attenuated the H_2O_2-induced increase in cell lethality (Matsui et al., 2010). Therefore, the effect of TPEN on the captan-induced cytotoxicity was also examined. The treatment with 30 μM captan for 3 h greatly increased the lethality (Figs. 1B and 7). In the presence of 10 μM TPEN, the increase in cell lethality by 30 μM captan was reduced (Fig. 7). Thus, Zn^{2+} is partly involved in the cytotoxicity of captan.

(Figure 7 near here)

4. Discussion

4.1. Captan-induced cell death and possible reciprocal changes in the cellular parameters

The cell death induced by 30 μM captan was associated with a decrease in cell size (cell shrinkage) and an increase in cell density (Fig. 1). Large population of living cells treated with captan was positive for annexin V before cell death (Fig. 2). The fact that such phenomenon precedes captan-induced cell death suggests that the nature of captan-induced cell death is

apoptotic rather than necrotic (Becila et al., 2017).

Captan increased $[Ca^{2+}]i$ by increasing the membrane permeability to Ca^{2+} (Fig. 3) and $[Zn^{2+}]i$ by increasing the release of intracellular Zn^{2+} (Fig. 4). Sustained increases in both $[Ca^{2+}]i$ and $[Zn^{2+}]i$ may disrupt intracellular signaling because both Ca^{2+} and Zn^{2+} are recognized as intracellular messengers (Bagur and Hajnóczky, 2017; Chabosseau et al., 2018). Furthermore, abnormal increases in $[Ca^{2+}]i$ and $[Zn^{2+}]i$ are associated with oxidative stress (Matsui et al., 2010; Gangwar et al., 2017) and cell death (Kumari et al., 2017; Shimoji et al., 2017; Parys and Bultynck, 2018). Captan-induced decrease in [NPT]i and increase in $[O_2^-]i$ (Fig. 5) resulted in the augmentation of oxidative stress, which consequently increased the cell vulnerability to oxidative stress elicited by 300 μM H_2O_2 (Fig. 6). Oxidative stress elevates both $[Ca^{2+}]i$ and $[Zn^{2+}]i$ (Abiria et al., 2017; Furuta et al., 2017) and $ZnCl_2$ may elevate the cytotoxicity of H_2O_2 by increasing the $[Zn^{2+}]i$ (Matsui et al., 2010), suggesting a reciprocal correlation between $[Zn^{2+}]i$ and oxidative stress (Matsui et al., 2010) and an inverse correlation between [NPT]i and $[Zn^{2+}]i$ (Kinazaki et al., 2009). Despite the difficulty to exactly determine the trigger of captan cytotoxicity and the mechanism for captan-induced potentiation of H_2O_2 cytotoxicity, the present study showed a correlation between captan-induced changes in the cellular parameters and oxidative stress. Some results confirm the results of Suzuki et al. (2004) although the concentrations of captan were lower in this study.

4.2. Toxicological implication

Because the *in vitro* concentrations of captan used in this study to induce cell death were higher than the urinary biomarker concentrations of captan in adults and children residing near agricultural land in Britain (Galea et al., 2015) and the plasma concentrations of

tetrahydrophthalimide (one of main metabolites of captan) in volunteers orally administered captan (Berthet et al., 2012), captan is considered unlikely to induce cell death in the daily lives of humans. However, the levels of captan residue detected in apples with no post-harvest preparation ranged from 0.02 mg/kg (minimum) to 3.0-5.1 mg/kg (maximum) (Rawn et al., 2008; Lozowicka, 2015), suggesting that high concentration of captan can reach the areas where the apples are distributed, even though the exact concentration of captan in the residue has not been calculated. The fact that the concentrations of captan that induce necrotic and apoptotic cell death in *Saccharomyces* cerevisiae (Scariot et al., 2017) are similar to those in rat lymphocytes (Figs. 1 and 2), and the concentrations of captan that increase the $[Ca^{2+}]i$ and $[Zn^{2+}]i$ in rat lymphocytes were 10-30 μM (Figs. 3 and 4), indicate that captan at environmental levels may affect the $[Ca^{2+}]i$, $[Zn^{2+}]i$, and [NPT]i in wild organisms, resulting in adverse effects.

Conflict of interest

All authors affirm that there are no conflicts of interest to declare.

Acknowledgements

This study was supported by Grant-in-Aids for Scientific Research (C26340039) from the Japan Society for the Promotion of Science.

References

Abbott, C.P., Beckerman, J.L., 2018. Incorporating adjuvants with captan to manage common apple diseases. Plant Disease, 102(1), 231–236.

Abiria, S.A., Krapivinsky, G., Sah, R., Santa-Cruz, A.G., Chaudhuri, D., Zhang, J., Adstamongkonkul, P., DeCaen, P.G., Clapham, D.E., 2017. TRPM7 senses oxidative stress to release Zn^{2+} from unique intracellular vesicles. Proceedings of the National Academy of Sciences, 114(30), E6079–E6088.

Arce, G.T., Gordon, E.B., Cohen, S.M., Singh, P., 2010. Genetic toxicology of folpet and captan. Critical Reviews in Toxicology, 40(6), 546–574.

Bagur, R., Hajnóczky, G., 2017. Intracellular Ca^{2+} sensing: its role in calcium homeostasis and signaling. Molecular Cell, 66(6), 780–788.

Becila, S., Boudida, Y., Gagaoua, M., Hafid, K., Boudchicha, H., Smili, H., Belachehabe, R., Herrera-Mendez, C.H., Sentandreu, M.A., Labas, R., Astruc, T., Boudjellal, A., Picard, B., Ouali, A., 2017. Cells shrinkage and phosphatidylserine externalization in post mortem muscle by fluorescence microscopy. In 3rd International Multidisciplinary Microscopy and Microanalysis Congress (InterM) (pp. 53–63). Cham, Switzerland: Springer.

Berthet, A., Bouchard, M. Danuser, B., 2012. Toxicokinetics of captan and folpet biomarkers in orally exposed volunteers. Journal of Applied Toxicology, 32(3), 194–201.

Bhosale, G., Sharpe, J.A., Sundier, S.Y., Duchen, M.R., 2015. Calcium signaling as a mediator of cell energy demand and a trigger to cell death. Annals of the New York Academy of Sciences, 1350(1), 107–116.

Chabosseau, P., Cheung, R., Woodier, J., Rutter, G.A., 2018. Sensors for measuring subcellular zinc pools. Metallomics, 10, 229–239.

Chikahisa. L., Oyama, Y., Okazaki, E., Noda, K., 1996. Fluorescent estimation of H_2O_2-induced changes in cell viability and cellular nonprotein thiol level of dissociated rat thymocytes. Japanese Journal of Pharmacology, 71, 299–305.

Dalvi, R.R., 1988. Involvement of glutathione in the reduction of captan‐induced in vivo inhibition of monooxygenases and liver toxicity in the rat. Journal of Environmental Science & Health Part B, 23(2), 171–178.

DeMarsay, A., 2012. Guidelines for developing an effective fungicide spray program for wine grapes in Maryland 2012. http://marylandgrapes.org/growing/FungicideSprayProgramGuide2012.pdf

Furuta, T., Mukai, A., Ohishi, A., Nishida, K., Nagasawa, K., 2017. Oxidative stress-induced increase of intracellular zinc in astrocytes decreases their functional expression of P2X7 receptors and engulfing activity. Metallomics, 9(12), 1839–1851.

Galea, K.S., MacCalman, L., Jones, K., Cocker, J., Teedon, P., Cherrie, J.W., Van Tongeren, M., 2015. Urinary biomarker concentrations of captan, chlormequat, chlorpyrifos and cypermethrin in UK adults and children living near agricultural land. Journal of Exposure Science and Environmental Epidemiology, 25(6), 623–631.

Gangwar, R., Meena, A. S., Shukla, P. K., Nagaraja, A. S., Dorniak, P. L., Pallikuth, S., Waters, C.M., Sood, A., Rao, R., 2017. Calcium-mediated oxidative stress: a common mechanism in tight junction disruption by different types of cellular stress. Biochemical Journal, 474(5), 731–749.

Gee, K.R., Zhou, Z.L., Qian, W.J., Kennedy, R., 2002. Detection and imaging of zinc secretion from pancreatic beta-cells using a new fluorescent zinc indicator. Journal of the American Chemical Society, 124, 776–778.

Hashimoto, E., Oyama, T.B., Oyama, K., Nishimura, Y., Oyama, T.M., Ueha-Ishibashi, T., Okano, Y., Oyama, Y., 2009. Increase in intracellular Zn^{2+} concentration by thimerosal in rat thymocytes: Intracellular Zn^{2+} release induced by oxidative stress. Toxicology in Vitro, 23(6), 1092–1099.

Kao, J.P., Harootunian, A.T, Tsien, R.Y., 1989. Photochemically generated cytosolic calcium pulses and their detection by fluo-3. Journal of Biological Chemistry, 264, 8179–8184.

Kawanai, T., Satoh, M., Murao, K., Oyama, Y., 2009. Methylmercury elicits intracellular Zn^{2+} release in rat thymocytes: its relation to methylmercury-induced decrease in cellular thiol content. Toxicology Letters, 191(2–3), 231–235.

Kinazaki A, Sakanashi Y, Oyama TM, Shibagaki H, Yamashita K, Hashimoto E, Nishimura Y, Ishida S, Okano Y, Oyama Y., 2009. Micromolar Zn^{2+} potentiates the cytotoxic action of submicromolar econazole in rat thymocytes: possible disturbance of intracellular Ca^{2+} and Zn^{2+} homeostasis. Toxicology In Vitro, 23, 610–616.

Kocyła, A., Adamczyk, J., Krężel, A., 2018. Interdependence of free zinc changes and protein complex assembly–insights into zinc signal regulation. Metallomics, 10(1), 120–131.

Koopman, G., Reutelingsperger, C.P., Kuijten, G.A., Keehnen, R.M., Pals, S.T., Van Oers, M.H., 1994. Annexin V for flow cytometric detection of phosphatidylserine expression on B cells undergoing apoptosis. Blood, 84, 1415–1420.

Kumari, A., Singh, K.P., Mandal, A., Paswan, R.K., Sinha, P., Das, P., Ali, V., Bimal, S., Lal,

C.S., 2017. Intracellular zinc flux causes reactive oxygen species mediated mitochondrial dysfunction leading to cell death in Leishmania donovani. PLoS One, 12(6):e0178800.

Lozowicka, B., 2015. Health risk for children and adults consuming apples with pesticide residue. Science of the Total Environment, 502, 184-198.

Lukens, R.J., 2013. Chemistry of fungicidal action (Vol. 10). New York, USA: Springer Science & Business Media.

Maeda, H., Yamamoto, K., Nomura, Y., Kohno, I., Hafsi, L., Ueda, N., Yoshida, S., Fukuda, M., Fukuyasu, Y., Yamauchi, Y., Itoh, N., 2005. A design of fluorescent probes for superoxide based on a nonredox mechanism. Journal of the American Chemical Society, 127(1), 68–69.

Maret, W., 1994. Oxidative metal release from metallothionein via zinc-thiol/disulfide interchange. Proceedings of the National Academy of Sciences, 91(1), 237–241.

Matsui, H., Oyama, T.M., Okano, Y., Hashimoto, E., Kawanai, T., & Oyama, Y., 2010. Low micromolar zinc exerts cytotoxic action under H_2O_2-induced oxidative stress: Excessive increase in intracellular Zn^{2+} concentration. Toxicology, 276, 27–32.

Parys J.B., Bultynck, G., 2018. Ca^{2+} signaling and cell death: Focus on the role of Ca^{2+} signals in the regulation of cell death & survival processes in health, disease and therapy. Cell Calcium, 70, 1–2.

Pesticide National Synthesis Project, US Geological Survey, 2018. Pesticide Use Maps - Captan https://water.usgs.gov/nawqa/pnsp/usage/maps/show_map.php?year=2015&map=CAPTAN&hilo=L&disp=Captan

Rawn, D.F., Quade, S.C., Sun, W.F., Fouguet, A., Bélanger, A., Smith, M., 2008. Captan

residue reduction in apples as a result of rinsing and peeling. Food Chemistry, 109(4), 790–796.

Scariot, F.J., Jahn, L., Delamare, A.P.L., Echeverrigaray, S., 2017. Necrotic and apoptotic cell death induced by Captan on Saccharomyces cerevisiae. World Journal of Microbiology and Biotechnology, 33(8), 159.

Shimoji, M., Hara, H., Kamiya, T., Okuda, K., Adachi, T., 2017. Hydrogen sulfide ameliorates zinc-induced cell death in neuroblastoma SH-SY5Y cells. Free Radical Research, 51(11–12), 978–985.

Slepchenko, K.G., Lu, Q., Li, Y.V., 2017. Cross talk between increased intracellular zinc (Zn^{2+}) and accumulation of reactive oxygen species in chemical ischemia. American Journal of Physiology-Cell Physiology, 313(4), C448–C459.

Suzuki, T., Nojiri, H., Isono, H., Ochi, T., 2004. Oxidative damages in isolated rat hepatocytes treated with the organochlorine fungicides captan, dichlofluanid and chlorothalonil. Toxicology, 204, 97–107.

Figure legends

Figure 1. Captan-induced changes in population of cells exhibiting propidium fluorescence, forward scatter, and side scatter of rat thymic lymphocytes. The cells were treated with captan for 3 h. (A) Captan-induced changes in cytogram (forward scatter intensity versus propidium fluorescent intensity), which was constructed with 2500 cells. (B) Captan-induced change in cell lethality (percentage population of propidium-stained cells). (C) Captan-induced changes in forward and side scatter intensities. Column and bar indicate mean and standard deviation of four samples, respectively. Asterisks (*, **) show significant difference ($P < 0.05$, 0.01) between the control group (CONTROL) and the captan-treated cells.

Figure 2. Captan-induced change in population (N, A, P, and AP) of cells classified with propidium iodide and annexin V-FITC. The cells were treated with captan for 1 h and then the cells were further incubated with propidium iodide and annexin V-FITC for 0.5 h to assess the process of cell death. (A) Captan-induced changes in cytogram (propidium fluorescence versus FITC fluorescence), which was constructed with 2500 cells. N = intact living cells, A= annexin V-positive living cells, P = annexin V-negative dead cells, PA = annexin V-positive dead cells. (B) Captan-induced changes in the population described in (A). Column and bar indicate mean and standard deviation of four samples, respectively. Asterisks (*, **) show significant difference ($P < 0.05$, 0.01) between the control group (CONTROL) and the captan-treated cells.

Figure 3. Captan-induced increase in the intensity of Fluo-3 fluorescence. The cells were treated with 1–30 μM captan for 1 h. (A) Concentration-dependent increase in the intensity induced by captan. (B) Captan-induced change in Fluo-3 fluorescence under external Ca^{2+}-free condition. Column and bar indicate mean and standard deviation of four samples, respectively.

Asterisks (**) show significant difference ($P < 0.01$) between the control group (CONTROL) and the captan-treated cells. Symbols (##) indicate significant difference ($P < 0.01$) between the groups with and without Ca^{2+} (Ca-FREE).

Figure 4. Captan-induced increase in the intensity of FluoZin-3 fluorescence. The cells were treated with 1–30 μM captan for 1 h. (A) Concentration-dependent increase in the intensity induced by captan. (B) Captan-induced change of Fluo-3 fluorescence in the presence of Zn^{2+}-chelators (DTPA and TPEN). Column and bar indicate mean and standard deviation of four samples, respectively. Asterisks (**) show significant difference ($P < 0.01$) between the control group (CONTROL) and the captan-treated cells. Symbols (##) indicate significant difference ($P < 0.01$) between the groups without and with Zn^{2+} chelator (DTPA and TPEN).

Figure 5. Captan-induced changes in oxidative stress. The cells were treated with captan for 1 h and then the cells were incubated with 5-CMF-DA for 0.5 h. (A) Captan-induced changes in the intensity of 5-CMF fluorescence. (B) Captan-induced increase in the intensity of BES-SO fluorescence. Asterisks (**) show significant difference ($P < 0.01$) between the control group (CONTROL) and the captan-treated cells.

Figure 6. Captan-induced increase in the cytotoxicity of H_2O_2 and cell lethality. The cells were treated with captan, H_2O_2, or both for 3 h. Asterisks (*, **) show significant difference ($P < 0.05, 0.01$) between the control group (CONTROL) and the cells treated with captan and/or H_2O_2. Symbols (##) indicate significant difference ($P < 0.01$) between the H_2O_2-treated groups without and with captan.

Figure 7. Effect of TPEN on the cytotoxicity of captan. The cells were treated with 30 μM captan, 10 μM TPEN, or both for 3 h. Asterisks (**) show significant difference ($P < 0.01$)

between the control group (CONTROL) and the cells treated with 30 μM captan. Symbols (##) indicate significant difference ($P < 0.01$) between the captan-treated groups without and with TPEN.

Table 1. Specific reagents used in this study

A. Fluorescent probes [Manufacturer]	Emission Wavelength
Propidium Iodide (PI) [Molecular Probes, Inc., Eugene, OR, USA]	PI: 600 ± 20 nm
Annexin V-FITC [Molecular Probes]	FITC: 530 ± 20 nm
Fluo-3-AM [Dojin Chemical Laboratory, Kumamoto, Japan]	Fluo-3: 530 ± 20 nm
FluoZin-3-AM [Molecular Probes]	FluoZin-3: 530 ± 20 nm
BES-SO-AM [Wako Pure Chemicals, Osaka, Japan]	BES-SO: 530 ± 20 nm
5-Chloromethylfluorescein Diacetate (5-CMF-DA) [Molecular Probes]	5-CMF: 530 ± 20 nm

(*) Excitation wavelength was 488 nm for all fluorescent probes.

B. Zinc chelator [Manufacturer]	Purpose
Diethylenetriamine-N,N,N′,N″,N″-pentaacetic acid (DTPA) [Dojin Chemical Laboratory]	Chelating external Zn^{2+}
N,N,N′,N′-tetrakis(2-pyridylmethyl)ethylenediamine (TPEN) [Dojin Chemical Laboratory]	Chelating intracellular Zn^{2+}

Figure 1

(A)

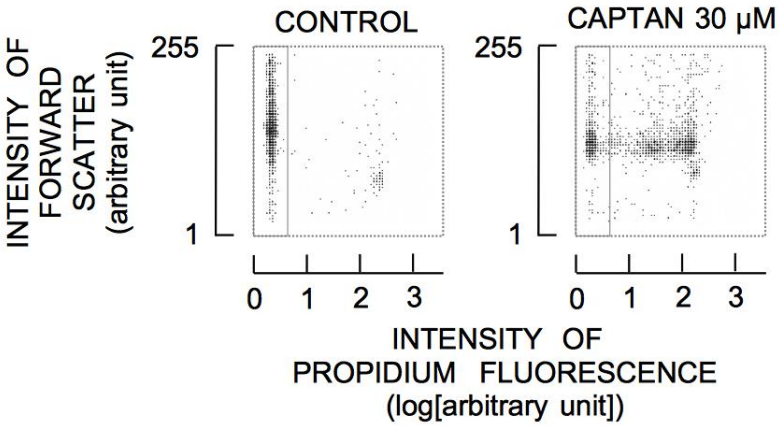
CONTROL
CAPTAN 30 μM
INTENSITY OF FORWARD SCATTER (arbitrary unit)
255
1
0 1 2 3
INTENSITY OF PROPIDIUM FLUORESCENCE (log[arbitrary unit])

(B)

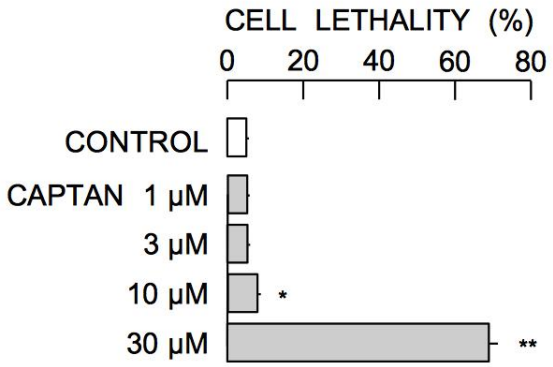
CELL LETHALITY (%)
0 20 40 60 80
CONTROL
CAPTAN 1 μM
3 μM
10 μM
30 μM
*
**

(C)

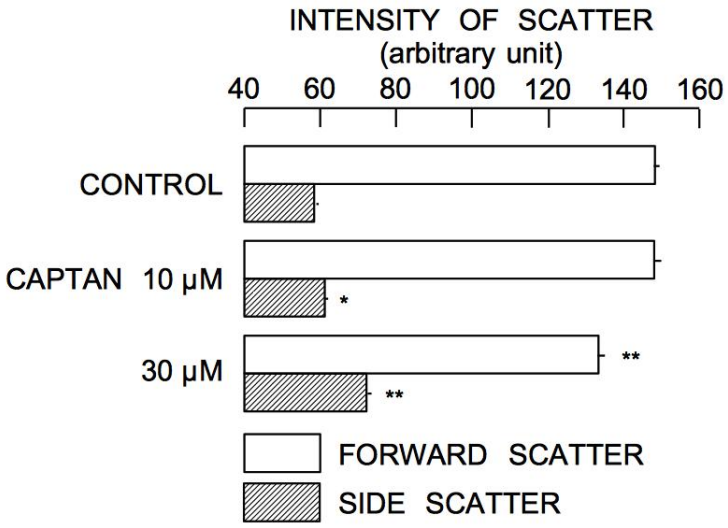
INTENSITY OF SCATTER (arbitrary unit)
40 60 80 100 120 140 160
CONTROL
CAPTAN 10 μM
30 μM
*
**
**
FORWARD SCATTER
SIDE SCATTER

Figure 2

(A)

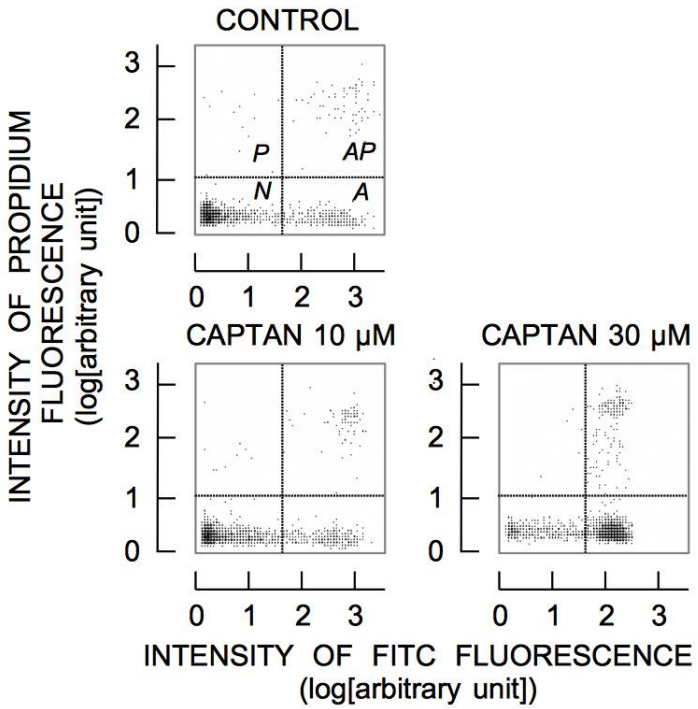
CONTROL
CAPTAN 10 μM
CAPTAN 30 μM
P
AP
N
A
0 1 2 3
INTENSITY OF PROPIDIUM FLUORESCENCE (log[arbitrary unit])
INTENSITY OF FITC FLUORESCENCE (log[arbitrary unit])

(B)

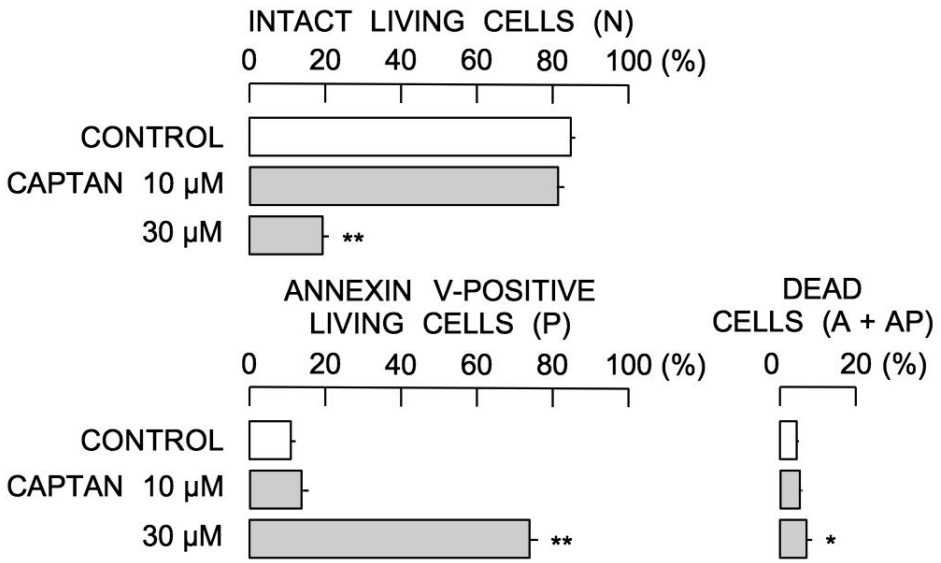
INTACT LIVING CELLS (N)
0 20 40 60 80 100 (%)
CONTROL
CAPTAN 10 μM
30 μM
**
ANNEXIN V-POSITIVE LIVING CELLS (P)
0 20 40 60 80 100 (%)
DEAD CELLS (A + AP)
0 20 (%)
CONTROL
CAPTAN 10 μM
30 μM
**
*

Figure 3

(A)

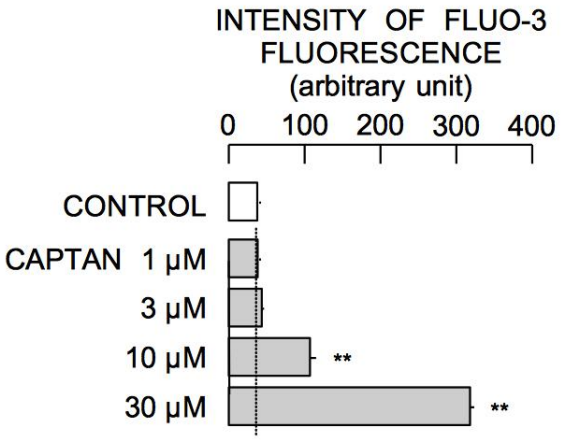
INTENSITY OF FLUO-3
FLUORESCENCE
(arbitrary unit)
0
100
200
300
400
CONTROL
CAPTAN 1 μM
3 μM
10 μM
30 μM
**
**

(B)

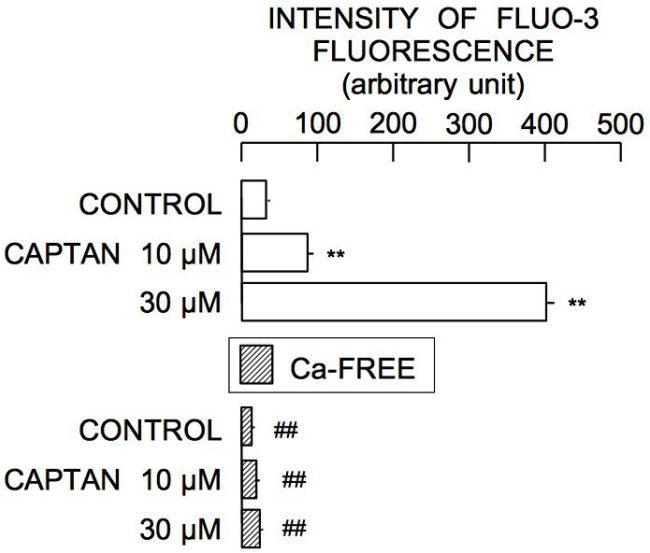
INTENSITY OF FLUO-3
FLUORESCENCE
(arbitrary unit)
0
100
200
300
400
500
CONTROL
CAPTAN 10 μM
30 μM
**
**
Ca-FREE
CONTROL
CAPTAN 10 μM
30 μM
##
##
##

Figure 4

(A)

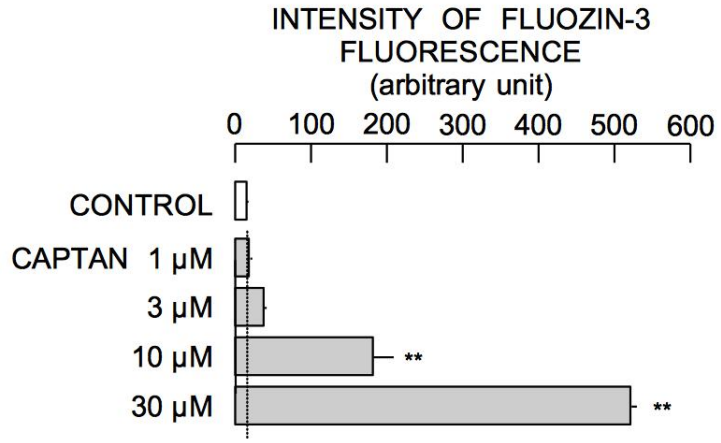
INTENSITY OF FLUOZIN-3
FLUORESCENCE
(arbitrary unit)
0 100 200 300 400 500 600
CONTROL
CAPTAN 1 μM
3 μM
10 μM
30 μM
**
**

(B)

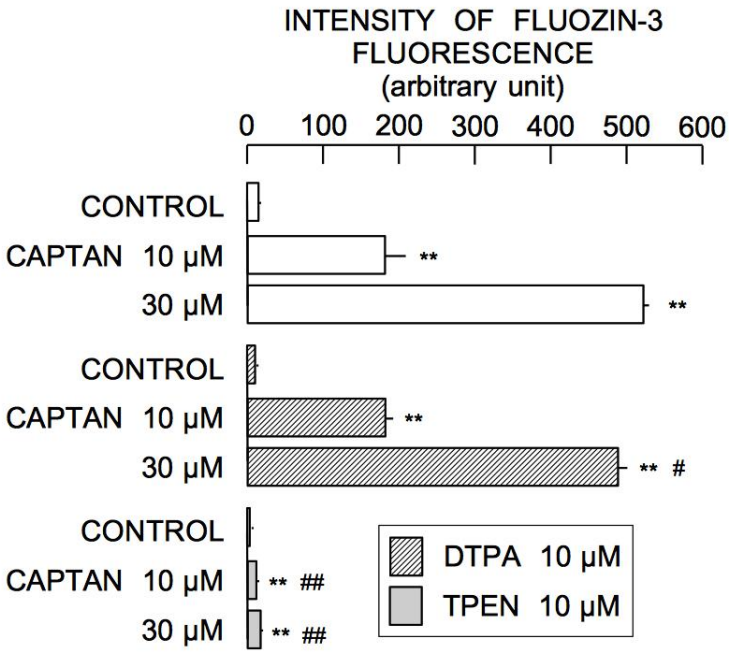
INTENSITY OF FLUOZIN-3
FLUORESCENCE
(arbitrary unit)
0 100 200 300 400 500 600
CONTROL
CAPTAN 10 μM
30 μM
**
**
CONTROL
CAPTAN 10 μM
30 μM
**
** #
CONTROL
CAPTAN 10 μM
30 μM
** ##
** ##
DTPA 10 μM
TPEN 10 μM

Figure 5

(A)

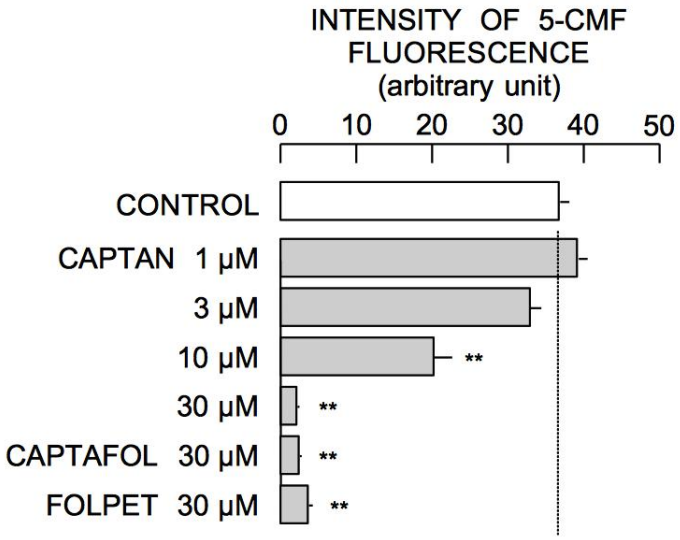
INTENSITY OF 5-CMF
FLUORESCENCE
(arbitrary unit)
0
10
20
30
40
50
CONTROL
CAPTAN 1 μM
3 μM
10 μM
30 μM
CAPTAFOL 30 μM
FOLPET 30 μM
**
**
**
**

(B)

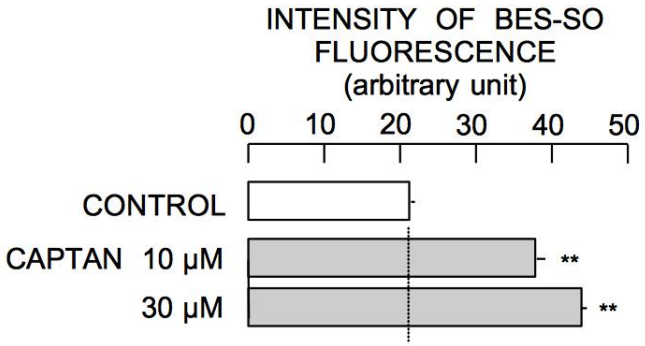
INTENSITY OF BES-SO
FLUORESCENCE
(arbitrary unit)
0
10
20
30
40
50
CONTROL
CAPTAN 10 μM
30 μM
**
**

Figure 6

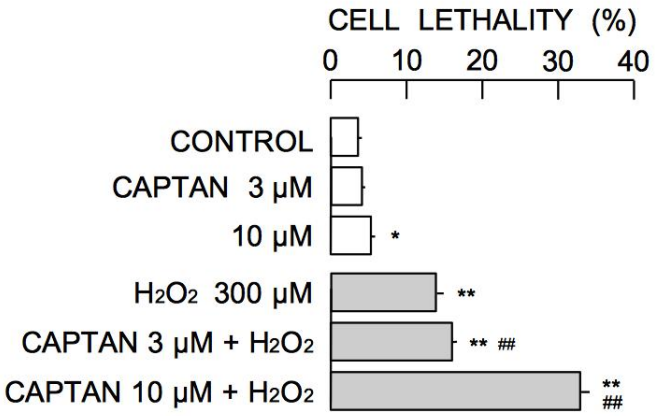
CELL LETHALITY (%)
0
10
20
30
40
CONTROL
CAPTAN 3 μM
10 μM
*
H2O2 300 μM
**
CAPTAN 3 μM + H2O2
** ##
CAPTAN 10 μM + H2O2
**
##

Figure 7

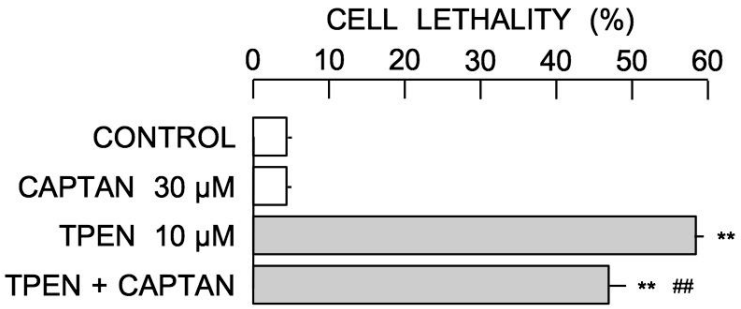
CELL LETHALITY (%)
0
10
20
30
40
50
60
CONTROL
CAPTAN 30 μM
TPEN 10 μM
TPEN + CAPTAN
**
** ##